ELSEVIER

Numerical implementation of the exact dynamics of free rigid bodies

Ramses van Zon *, Jeremy Schofield

Chemical Physics Theory Group, Department of Chemistry, University of Toronto, 80 Saint George Street, Toronto, ON, Canada M5S 3H6

Abstract

In this paper the exact analytical solution of the motion of a rigid body with arbitrary mass distribution is derived in the absence of forces or torques. The resulting expressions are cast into a form where the dependence of the motion on initial conditions is explicit and the equations governing the orientation of the body involve only real numbers. Based on these results, an efficient method to calculate the location and orientation of the rigid body at arbitrary times is presented. This implementation can be used to verify the accuracy of numerical integration schemes for rigid bodies, to serve as a building block for event-driven discontinuous molecular dynamics simulations of general rigid bodies, and for constructing symplectic integrators for rigid body dynamics.
© 2006 Elsevier Inc. All rights reserved.

1. Introduction

The importance of the dynamics of rigid bodies in physics and engineering has been recognized since the early 19th century. The early work of Euler, Hermite, Poisson, Jacobi and many others on exactly soluble systems lead to great advances in the field of applied mathematics as well as in mechanics. More recently, rigid hard spheres served as the first prototypical model for fluids treated by computer simulation [1]. Today, rigid bodies are used to model phenomena on a variety of different length scales: On molecular length scales, rigid bodies are used in the modeling of the microscopic dynamics of molecules in condensed phases [2–4], on a mesoscopic scale, they are used to construct simple models of polymers and other complex systems [5], while on a macroscopic level they play an important role in robotics. The dynamics of rigid bodies is also of relevance to the computer game industry, where many improvements in simulating rigid bodies have been

* Corresponding author. Tel.: +1 416 946 7044; fax: +1 416 978 5325.
E-mail address: rzon@chem.utoronto.ca (R. van Zon).

developed [6]. Finally, on an even larger scale, many astrophysical objects such as planets, satellites and space crafts can be regarded as rigid bodies on certain time scales [7,8].

According to the laws of classical mechanics, the motion of a rigid body consists of translation of the center of mass of the body and rotation of the orientation of the body about its center of mass. In the most general case in which the body is subject to forces and torques, an analytical solution of the dynamics is not possible and a numerical scheme is required to integrate the equations of motion. With the advent of powerful computers, much work has been devoted to finding stable and efficient integration schemes for rotating rigid bodies [9–12]. The use of numerical integrators is now so widespread that they are frequently used even in cases where an analytical solution of the dynamics is available. This is unfortunate, since an exact solution cannot only serve as a special case against which numerical integration schemes may be tested, but can also be directly used in so-called discontinuous molecular dynamics of rigid bodies, in which the bodies perform free motion in between interaction events. A hard sphere gas is the prototypical example of such a system. In these kinds of simulations, using an exact solution of the free dynamics yields an enormous computational benefit compared to having to integrate the free dynamics numerically (see e.g. Refs. [3 and 4]). Furthermore, for molecular dynamics of systems with a continuous potential, an exact solution is also often useful in constructing so-called symplectic integration schemes, and typically leads to enhanced stability [13,12,14,15].

Perhaps the principal reason why the analytical solution of the motion of a free rigid body is seldom used is that the general solution is simply not well-known. Many advanced textbooks in mechanics avoid discussing the motion of general rigid bodies, and only consider certain symmetric cases [16] in which the equations of motion are particularly simple. This probably is due to the fact that the general solution—apparently first found by Rueb [17] in 1834 and later completed by Jacobi in 1849 [18]—involves special functions, called elliptic and theta functions, which are perhaps less familiar than other special functions. Furthermore, even when the case of a general rotor is discussed [17–19,8,20], the treatment of its motion is often incomplete, in rather abstract form (using complex-valued functions) and presented in a special inertial coordinate frame rather than a general laboratory inertial frame.

The goal of this paper is to demonstrate that none of these issues needs to be an obstacle to the use of the exact solution of the equations of motion of an asymmetric rigid body in numerical work. It will first be shown that although the derivation of the general solution of the equations of motion of a rigid body requires a bit of complex analysis, the final result can be expressed without any reference to complex arithmetic. Secondly, the solution will be formulated in a general inertial frame and for general initial conditions of the rigid body. Finally, it will be shown that the special functions occurring in the solution can be numerically implemented in an efficient fashion. Based on these considerations, the numerical implementation of the (admittedly non-trivial) motion of an asymmetric rigid body in the absence of forces and torques is relatively straightforward.

The paper is organized as follows: In Section 2, the motion of a rigid body is reviewed starting in Section 2.1 with a brief overview of the properties of rigid bodies. Subsequently, in Section 2.2 the equations of motion are given, while in Section 2.3 these are specialized to the case of free motion. The novel part of the paper starts in Section 3, where a new derivation of the exact solution of the time dependence of the orientation of the body is given, first in general and then explicitly for the spherical top, the symmetric top and the asymmetric top (Sections 3.1–3.3, respectively). In Section 4, some further numerical issues are addressed. An example is given in Section 5 and the paper ends in Section 6 with a discussion of the results and their possible applications.

2. Review of the motion of rigid bodies

2.1. Rigid bodies

The shape of a rigid body is specified by the set of all material points $\{\tilde{\mathbf{r}}_i\}$ of the body. The points $\tilde{\mathbf{r}}_i = (\tilde{x}_i, \tilde{y}_i, \tilde{z}_i)$ are three-dimensional vectors with respect to a reference coordinate frame called the *body frame*, and constitute a reference orientation of the body [20]. Furthermore, a mass m_i is associated with each material point. The mass distribution of the body plays an important role in its dynamics.

Since any translation or rotation acting on all points $\tilde{\mathbf{r}}_i$ leaves the shape of the body unchanged, there is an arbitrariness in the choice of *body frame* which can be exploited. By a suitable translation, one may always set the center of mass to be in the origin, i.e.,

$$\sum_i m_i \tilde{\mathbf{r}}_i = 0. \tag{2.1}$$

Furthermore, using a suitable rotation, the moment of inertia tensor $\tilde{\mathbf{I}}$ can be brought to its principal form:

$$\tilde{\mathbf{I}} = \sum_i m_i \begin{pmatrix} \tilde{y}_i^2 + \tilde{z}_i^2 & -\tilde{x}_i\tilde{y}_i & -\tilde{x}_i\tilde{z}_i \\ -\tilde{x}_i\tilde{y}_i & \tilde{x}_i^2 + \tilde{z}_i^2 & -\tilde{y}_i\tilde{z}_i \\ -\tilde{x}_i\tilde{z}_i & -\tilde{y}_i\tilde{z}_i & \tilde{x}_i^2 + \tilde{y}_i^2 \end{pmatrix} = \begin{pmatrix} I_1 & 0 & 0 \\ 0 & I_2 & 0 \\ 0 & 0 & I_3 \end{pmatrix}. \tag{2.2}$$

For subsequent developments, it will be assumed that these transformations have been performed.

Because the body frame is fixed to the body, the material points $\tilde{r}_i$ are independent of time. However since the body itself moves through physical space, the location of each point $\tilde{r}_i$ in the physical coordinate system, or *lab frame*, must be determined as a function of time to describe its motion. The position of mass point i in the lab frame will be denoted by $\mathbf{r}_i(t) = (x_i(t), y_i(t), z_i(t))$. Since the body is rigid, its motion is a time-dependent orientation-and-distance-preserving transformation from the body frame to the lab frame. The most general such transformation is a combination of a translation and a rotation:

$$\mathbf{r}_i(t) = \mathbf{R}(t) + \mathbf{A}^\dagger(t)\tilde{\mathbf{r}}_i. \tag{2.3}$$

Here and below, matrix–vector and matrix–matrix products such as $\mathbf{A}^\dagger(t)\tilde{r}_i$ will be denoted implicitly, i.e, without a "·", which will only be used for inner products. For notational simplicity, the explicit time dependence will be omitted in most expressions, i.e., $\mathbf{r}_i(t)$ will be denoted simply by $\mathbf{r}_i$. Exceptions are if the time argument is equal to zero (e.g. $\mathbf{r}_i(0)$) or integrated over.

In Eq. (2.3), the vector $\mathbf{R}$ denotes the position of the center of mass at time t, while the orthogonal matrix $\mathbf{A}^\dagger$ represents the orientation of the body with respect to the center of mass at that time and is often called the *attitude matrix*. Note that $\mathbf{A}$ transforms vectors from the lab to the body frame, while its transpose $\mathbf{A}^\dagger$ transforms vectors from the body to the lab frame.

The motions of the different material points of a rigid body are obviously closely related. Instead of working with the (linear) velocities of all points, one can instead use a formulation of the dynamics that utilizes the angular velocity vector $\boldsymbol{\omega} = (\omega_1, \omega_2, \omega_3)$ of the body around its center of mass. This angular velocity vector is defined such that its direction coincides with the rotation axis and its magnitude coincides with the rate at which it rotates. As a consequence of this definition, the velocity of any point of the rigid body satisfies the standard relation [16]

$$\mathbf{v}_i = \mathbf{V} + \boldsymbol{\omega} \times (\mathbf{r}_i - \mathbf{R}), \tag{2.4}$$

where $\mathbf{V} = \dot{\mathbf{R}}$ is the velocity of the center of mass. Defining the antisymmetric matrix

$$\mathbf{W}(\boldsymbol{\omega}) = \begin{pmatrix} 0 & -\omega_3 & \omega_2 \\ \omega_3 & 0 & -\omega_1 \\ -\omega_2 & \omega_1 & 0 \end{pmatrix}, \tag{2.5}$$

and using Eqs. (2.3), (2.4) can also be written as

$$\mathbf{v}_i = \mathbf{V} + \mathbf{W}(\boldsymbol{\omega})\mathbf{A}^\dagger\tilde{\mathbf{r}}_i. \tag{2.6}$$

Taking the time derivative of Eq. (2.3) and using Eq. (2.6), one sees that ω and $\dot{\mathbf{A}}$ are related via

$$\dot{\mathbf{A}}^\dagger\mathbf{A} = \mathbf{W}(\boldsymbol{\omega}), \tag{2.7}$$

Given the central role of rotation matrices below, it is useful to establish some notation. A rotation matrix $\mathbf{U}$ is a special orthogonal matrix that can be specified by a rotation axis $\hat{\mathbf{n}} = (n_1, n_2, n_3)$ and an angle ψ. Here $\hat{\mathbf{n}}$ is a unit vector, so that one may also say that any non-unit vector $\psi\hat{\mathbf{n}}$ can be used to specify a rotation, where its norm is equal to the angle ψ and its direction is along the axis $\hat{\mathbf{n}}$. In fact, one can express this rotation matrix as $\mathbf{U}(\psi\hat{\mathbf{n}}) = \exp\mathbf{W}(\psi\hat{\mathbf{n}})$. The explicit form of this rotation matrix may be found using Rodrigues' formula [16].

2.2. Dynamics

It is clear from Eq. (2.3) that the motion of a rigid body as a function of time is determined by the time dependence of the center of mass vector $\boldsymbol{R}$ and the attitude matrix $\mathbf{A}$. According to the mechanics of rigid bodies, these follow from the equations of motion

$$F = \dot{P}, \quad \tau = \dot{L}. \tag{2.8}$$

Here, $\boldsymbol{F}$ is the sum of all forces acting on the body, $\boldsymbol{P} = M\boldsymbol{V}$ (with $M = \sum_i m_i$) is the total momentum, $\boldsymbol{\tau}$ the total torque with respect to the center of mass of the body and $\boldsymbol{L} = \mathbf{I}\boldsymbol{\omega}$ is the angular momentum. One may equivalently write

$$F = M\dot{V}, \quad \tau = \frac{\mathrm{d}}{\mathrm{d}t}(\mathbf{I}\omega). \tag{2.9}$$

The latter equation is more conveniently written in the body frame using $\tilde{\boldsymbol{\omega}} = \mathbf{A}\boldsymbol{\omega}$, $\tilde{\boldsymbol{\tau}} = \mathbf{A}\boldsymbol{\tau}$ and $\tilde{\mathbf{I}} = \mathbf{A}\mathbf{I}\mathbf{A}^{\dagger}$, which yields

$$\tilde{\tau} = \mathbf{A}\dot{\mathbf{A}}^{\dagger}\tilde{\mathbf{I}}\tilde{\omega} + \tilde{\mathbf{I}}\dot{\tilde{\omega}} = \mathbf{A}\mathbf{W}(\omega)\mathbf{A}^{\dagger}\tilde{\mathbf{I}}\tilde{\omega} + \tilde{\mathbf{I}}\dot{\tilde{\omega}} = \mathbf{W}(\tilde{\omega})\tilde{\mathbf{I}}\tilde{\omega} + \tilde{\mathbf{I}}\dot{\tilde{\omega}}, \tag{2.10}$$

where Eq. (2.7) was used to obtain the second equality, and the third equality was obtained using

$$\mathbf{A}\mathbf{W}(\omega)\mathbf{A}^{\dagger} = \mathbf{W}(\mathbf{A}\omega) = \mathbf{W}(\tilde{\omega}). \tag{2.11}$$

Writing out Eq. (2.10) in its components gives the so-called *Euler equations*. Solving these equations yields the time dependence of the angular velocities in the body frame. To consequently find the attitude matrix $\mathbf{A}$, one uses Eqs. (2.7) and (2.11) to find

$$\dot{\mathbf{A}} = -\mathbf{W}(\tilde{\omega})\mathbf{A}. \tag{2.12}$$

2.3. Force and torque-free case

In the special case where all external forces and torques are zero, i.e., $\boldsymbol{F} = 0$ and $\boldsymbol{\tau} = 0$, the equations of motion to solve simplify to

$$\dot{V} = 0, \quad \tilde{\mathbf{I}}\dot{\tilde{\omega}} = -\tilde{\omega} \times \tilde{\mathbf{I}}\tilde{\omega}, \quad \dot{\mathbf{A}} = -\mathbf{W}(\tilde{\omega})\mathbf{A}. \tag{2.13}$$

In the absence of forces and torques, the dynamics of the system is invariant under rotations and under translations in time and space. As a consequence of these symmetries, the energy E, momentum $\boldsymbol{P}$ and angular momentum $\boldsymbol{L}$ are conserved, where E is given by

$$E = E_{\mathrm{T}} + E_{\mathrm{R}} \tag{2.14}$$

with the translational and rotational energies equal to

$$\begin{aligned} E_{\mathrm{T}} &= \frac{1}{2M}|\boldsymbol{P}|^2 = \frac{1}{2}M|\boldsymbol{V}|^2, \\ E_{\mathrm{R}} &= \frac{1}{2}\boldsymbol{L}\cdot\mathbf{I}^{-1}\boldsymbol{L} = \frac{1}{2}\boldsymbol{\omega}\cdot\mathbf{I}\boldsymbol{\omega} = \frac{1}{2}\tilde{\boldsymbol{\omega}}\cdot\tilde{\mathbf{I}}\tilde{\boldsymbol{\omega}} = \frac{1}{2}(I_1\tilde{\omega}_1^2 + I_2\tilde{\omega}_2^2 + I_3\tilde{\omega}_3^2), \end{aligned} \tag{2.15}$$

respectively.

The time dependence of the translational part of the motion follows from the equation of motion $\dot{V} = 0$, which is easily solved to obtain

$$\begin{aligned} V &= V(0), \\ R &= R(0) + V(0)t. \end{aligned} \tag{2.16}$$

Since $\boldsymbol{V}(t) = \boldsymbol{V}(0)$, the translational energy E_{T} is conserved in the dynamics, which, in turn, implies that the rotational energy E_{R} is also conserved.

To solve the rotational equations of motion is less trivial. One has to solve the middle equation of (2.13), which, written out in components, reads

$$I_1\dot{\tilde{\omega}}_1 = \tilde{\omega}_2\tilde{\omega}_3(I_2 - I_3),$$
$$I_2\dot{\tilde{\omega}}_2 = \tilde{\omega}_3\tilde{\omega}_1(I_3 - I_1), \tag{2.17}$$
$$I_3\dot{\tilde{\omega}}_3 = \tilde{\omega}_1\tilde{\omega}_2(I_1 - I_2).$$

The general solution of this set of equations will be presented below. Given this solution, the remaining task is to determine the attitude matrix **A** from Eq. (2.12).

Although the general solution for **A** is hard to find in any textbook, it can be found in Jacobi's treatise on rigid body motion from 1849 [18]. Unfortunately, for mathematical elegance, the attitude matrix was only specified up to a rotation at a uniform speed which was not clearly identified, so that its numerical implementation is not altogether clear. Furthermore, Jacobi's derivation relies heavily on geometric arguments and Euler angles, which often pose problems in numerical applications. For this reason, the next section contains a novel derivation of the exact solution of **A** without reference to Euler angles, leading to an expression which is more readily implemented.

3. Exact solution of the attitude matrix in the absence of torques

While discussions of how to solve the Euler equations in the body frame are common, one rarely sees any mention of how to go about integrating the equation for the attitude matrix. Therefore, we have chosen to treat this derivation in a bit more detail than one would perhaps expect from a computational paper. First the general form of the solution will be derived, after which the three different case of rigid bodies are explicitly considered: spherical bodies (Section 3.1), symmetric tops (Section 3.2), and asymmetric tops (Section 3.3).

To obtain the general form of the attitude matrix **A**, we have to solve Eq. (2.12). Since this is a linear equation, its solution can be written in the form

$$\mathbf{A} = \mathbf{P}\mathbf{A}(0). \tag{3.1}$$

Here, **P** is a time-dependent matrix which also satisfies Eq. (2.12), but with initial condition $\mathbf{P}(0) = \mathbf{1}$. This corresponds to a case in which the body and lab frame initially coincide, i.e., in which the body is in the "upright" position. In this upright lab frame, the angular momentum vector is given by

$$\boldsymbol{L} = \begin{pmatrix} L_1 \\ L_2 \\ L_3 \end{pmatrix} = \tilde{\boldsymbol{L}}(0). \tag{3.2}$$

It will prove to be more convenient to work in a different lab frame, called the *invariant frame* (with vectors in this frame denoted by primed quantities), in which the angular momentum vector is along the z-axis and is equal to $\boldsymbol{L}' = (0,0,L)^\dagger$. Such a frame can be found by performing a rotation of the original frame through a rotation matrix $\mathbf{T}_1'^\dagger(0)$ (the reason for the peculiar notation will become clear below). This rotation is not unique and can be chosen such that one first rotates around the z-axis until the rotated angular momentum vector no longer has a y-component, and then subsequently rotates around the y-axis to remove the x-component of the angular momentum vector as well. Denoting $\tilde{L}_\perp = [\tilde{L}_1^2 + \tilde{L}_2^2]^{1/2}$, the combined rotation is easily shown to be [1]

$$\mathbf{T}_1'^\dagger(0) = \underbrace{\begin{pmatrix} \frac{\tilde{L}_3(0)}{L} & 0 & -\frac{\tilde{L}_\perp(0)}{L} \\ 0 & 1 & 0 \\ \frac{\tilde{L}_\perp(0)}{L} & 0 & \frac{\tilde{L}_3(0)}{L} \end{pmatrix}}_{\text{rotation to get } L_x'(0)=0} \underbrace{\begin{pmatrix} \frac{\tilde{L}_1(0)}{\tilde{L}_\perp(0)} & \frac{\tilde{L}_2(0)}{\tilde{L}_\perp(0)} & 0 \\ -\frac{\tilde{L}_2(0)}{\tilde{L}_\perp(0)} & \frac{\tilde{L}_1(0)}{\tilde{L}_\perp(0)} & 0 \\ 0 & 0 & 1 \end{pmatrix}}_{\text{rotation to get } L_y'(0)=0} = \begin{pmatrix} \frac{\tilde{L}_1(0)\tilde{L}_3(0)}{\tilde{L}_\perp(0)L} & \frac{\tilde{L}_2(0)\tilde{L}_3(0)}{L\tilde{L}_\perp(0)} & -\frac{\tilde{L}_\perp(0)}{L} \\ -\frac{\tilde{L}_2(0)}{\tilde{L}_\perp(0)} & \frac{\tilde{L}_1(0)}{\tilde{L}_\perp(0)} & 0 \\ \frac{\tilde{L}_1(0)}{L} & \frac{\tilde{L}_2(0)}{L} & \frac{\tilde{L}_3(0)}{L} \end{pmatrix}. \tag{3.3}$$

---

[1] For the special case when $\tilde{L}_\perp(0) = 0$ one may take $\mathbf{T}_1'(0) = \mathrm{diag}(\pm 1, 1, \pm 1)$ where the sign is chosen according to $\tilde{L}_3(0)/L = \pm 1$, i.e., depending on whether in the original lab frame $\boldsymbol{L}$ pointed in the positive or the negative z-direction.

This rotation is defined such that if $\boldsymbol{v}$ is a vector in the original lab frame, then $\boldsymbol{v}' = \mathbf{T}_1'^{\dagger}(0)\boldsymbol{v}$ is the corresponding vector in the invariant frame. To find the matrix corresponding to $\mathbf{P}$ in this new frame, note that since $\mathbf{P}$ relates vectors to the body frame through $\tilde{\boldsymbol{v}} = \mathbf{P}\boldsymbol{v}$, so that $\tilde{\boldsymbol{v}} = \mathbf{P}\mathbf{T}_1'(0)\boldsymbol{v}' = \mathbf{P}'\boldsymbol{v}'$, one can identify

$$\mathbf{P}' = \mathbf{P}\mathbf{T}_1'(0). \tag{3.4}$$

Since $\mathbf{T}_1'(0)$ is a constant matrix multiplying on the right, $\mathbf{P}'$ also satisfies Eq. (2.12) with initial condition $\mathbf{P}'(0) = \mathbf{T}_1'(0)$.

The convenience of this choice of frame becomes clear when $\mathbf{P}'$ is written in terms of its columns,

$$\mathbf{P}' = [\hat{\boldsymbol{u}}_1\hat{\boldsymbol{u}}_2\hat{\boldsymbol{u}}_3] \tag{3.5}$$

and one notes that

$$\hat{\boldsymbol{u}}_3 = \mathbf{P}' \begin{pmatrix} 0 \\ 0 \\ 1 \end{pmatrix} = \frac{\mathbf{P}'\boldsymbol{L}'}{L} = \frac{\tilde{\boldsymbol{L}}}{L}, \tag{3.6}$$

the components of which are known once the Euler equations are solved. Thus, by this choice of frame, one is able to determine the third column of the matrix $\mathbf{P}'$.

The remaining elements of $\mathbf{P}'$ can all be expressed in terms of a single time-dependent angle ψ. This is due to the orthogonality of $\mathbf{P}'$, which implies that the other two columns $\hat{\boldsymbol{u}}_1$ and $\hat{\boldsymbol{u}}_2$ must lie in a plane orthogonal to $\hat{\boldsymbol{u}}_3$ and must also be orthogonal to each other. Denoting $\hat{\boldsymbol{e}}_1$ and $\hat{\boldsymbol{e}}_2$ as two chosen orthogonal unit-vectors in this plane, one can therefore write

$$\hat{\boldsymbol{u}}_1 = \hat{\boldsymbol{e}}_1 \cos\psi - \hat{\boldsymbol{e}}_2 \sin\psi, \tag{3.7}$$

$$\hat{\boldsymbol{u}}_2 = \hat{\boldsymbol{e}}_1 \sin\psi + \hat{\boldsymbol{e}}_2 \cos\psi, \tag{3.8}$$

where the unit-vectors $\hat{\boldsymbol{e}}_1$ and $\hat{\boldsymbol{e}}_2$ are chosen to be:[2]

$$\hat{\boldsymbol{e}}_2 = \frac{\hat{\boldsymbol{e}}_z \times \hat{\boldsymbol{u}}_3}{|\hat{\boldsymbol{e}}_z \times \hat{\boldsymbol{u}}_3|} = \frac{\hat{\boldsymbol{e}}_z \times \tilde{\boldsymbol{L}}}{|\hat{\boldsymbol{e}}_z \times \tilde{\boldsymbol{L}}|} = \begin{pmatrix} -\frac{\tilde{L}_2}{\tilde{L}_\perp} \\ \frac{\tilde{L}_1}{\tilde{L}_\perp} \\ 0 \end{pmatrix}, \tag{3.9}$$

$$\hat{\boldsymbol{e}}_1 = \hat{\boldsymbol{e}}_2 \times \hat{\boldsymbol{u}}_3 = \begin{pmatrix} \frac{\tilde{L}_1\tilde{L}_3}{L\tilde{L}_\perp} \\ \frac{\tilde{L}_2\tilde{L}_3}{L\tilde{L}_\perp} \\ -\frac{\tilde{L}_\perp}{L} \end{pmatrix}, \tag{3.10}$$

where $\hat{\boldsymbol{e}}_z = (0,0,1)$, and we have used the fact that $|\hat{\boldsymbol{e}}_z \times \tilde{\boldsymbol{L}}| = (\tilde{L}_1^2 + \tilde{L}_2^2)^{1/2} = \tilde{L}_\perp$. Other choices of orthogonal unit-vectors $\hat{\boldsymbol{e}}_1$ and $\hat{\boldsymbol{e}}_2$ change the as-of-yet undetermined time-dependent angle ψ by a time independent offset. The current choice has the advantage that the matrix $[\hat{\boldsymbol{e}}_1(0)\ \hat{\boldsymbol{e}}_2(0)\ \hat{\boldsymbol{u}}_3(0)]$ is identical to $\mathbf{T}_1'(0)$, so that $\mathbf{P}'(0) = \mathbf{T}_1'(0)$, and hence

$$\psi(0) = 0. \tag{3.11}$$

Using Eqs. (3.7) and (3.8), $\mathbf{P}'$ has effectively been written as a product of two rotation matrices,

$$\mathbf{P}' = \mathbf{T}_1'\mathbf{T}_2', \tag{3.12}$$

where

$$\mathbf{T}_1' = [\hat{\boldsymbol{e}}_1\hat{\boldsymbol{e}}_2\hat{\boldsymbol{u}}_3] = \begin{pmatrix} \frac{\tilde{L}_1\tilde{L}_3}{L\tilde{L}_\perp} & -\frac{\tilde{L}_2}{\tilde{L}_\perp} & \frac{\tilde{L}_1}{L} \\ \frac{\tilde{L}_2\tilde{L}_3}{L\tilde{L}_\perp} & \frac{\tilde{L}_1}{\tilde{L}_\perp} & \frac{\tilde{L}_2}{L} \\ -\frac{\tilde{L}_\perp}{L} & 0 & \frac{\tilde{L}_3}{L} \end{pmatrix}, \tag{3.13}$$

---

[2] For the special case when $\tilde{L}_\perp = 0$ one may take $\hat{\boldsymbol{e}}_2 = (0,1,0)^{\dagger}$ and $\hat{\boldsymbol{e}}_1 = \hat{\boldsymbol{e}}_2 \times \hat{\boldsymbol{u}}_3$.

$$\mathbf{T}_2' = \begin{pmatrix} \cos\psi & \sin\psi & 0 \\ -\sin\psi & \cos\psi & 0 \\ 0 & 0 & 1 \end{pmatrix} = \mathbf{U}(-\psi\hat{\mathbf{z}}). \tag{3.14}$$

Note that $\mathbf{T}_1'$ in Eq. (3.13) is a rotation matrix because $\hat{\mathbf{e}}_1$, $\hat{\mathbf{e}}_2$ and $\hat{\mathbf{u}}_3$ form an orthogonal set by their construction in Eqs. (3.9) and (3.10). The matrix $\mathbf{P}$ can therefore be written as

$$\mathbf{P} = \mathbf{T}_1' \mathbf{T}_2' \mathbf{T}_1'^{\dagger}(0). \tag{3.15}$$

For the special cases of the spherical top and symmetric top, it is more convenient to express $\mathbf{P}$ as a product of two rotation matrices (implicitly also found in Ref. [8]):

$$\mathbf{P} = \mathbf{T}_1 \mathbf{T}_2, \tag{3.16}$$

where

$$\mathbf{T}_1 = \mathbf{T}_1' \mathbf{T}_1'^{\dagger}(0), \tag{3.17}$$

$$\mathbf{T}_2 = \mathbf{T}_1'(0) \mathbf{T}_2' \mathbf{T}_1'^{\dagger}(0). \tag{3.18}$$

Note that $\mathbf{T}_1$ and $\mathbf{T}_1'$ are determined by the solution of the Euler equations and require no further manipulations once the general solution of $\tilde{\mathbf{L}}$ is known.

Turning next to the matrix $\mathbf{T}_2$, noting that for any rotation $\mathbf{R}$ and vector $\mathbf{x}$, $\mathbf{R}\mathbf{U}(\mathbf{x})\mathbf{R}^{\dagger} = \mathbf{U}(\mathbf{R}\mathbf{x})$ and that $\mathbf{T}_1'(0)\hat{\mathbf{z}} = \tilde{\mathbf{L}}(0)/L$, the matrix $\mathbf{T}_2$ can written as a rotation by an angle of $-\psi$ around the axis $\tilde{\mathbf{L}}(0)/L$, i.e., using Eqs. (3.14) and (3.18),

$$\mathbf{T}_2 = \mathbf{U}(-\psi\tilde{\mathbf{L}}(0)/L). \tag{3.19}$$

The final task to determine $\mathbf{P}$ consists of deriving a differential equation for the time-dependent angle ψ and solving it subject to the initial condition $\psi(0) = 0$ (cf. Eq. (3.11)). To obtain this differential equation, note that from Eqs. (2.12), (2.7) and (3.5), it follows that

$$\dot{\hat{\mathbf{u}}}_1 = -\tilde{\boldsymbol{\omega}} \times \hat{\mathbf{u}}_1,$$

and hence from Eq. (3.7) one finds

$$\dot{\hat{\mathbf{e}}}_1 \cos\psi - \hat{\mathbf{e}}_1 \dot{\psi} \sin\psi - \dot{\hat{\mathbf{e}}}_2 \sin\psi - \hat{\mathbf{e}}_2 \dot{\psi} \cos\psi = -\tilde{\boldsymbol{\omega}} \times \hat{\mathbf{e}}_1 \cos\psi + \tilde{\boldsymbol{\omega}} \times \hat{\mathbf{e}}_2 \sin\psi.$$

Taking the inner product with $\hat{\mathbf{e}}_2$, using that $\hat{\mathbf{e}}_2 \cdot \dot{\hat{\mathbf{e}}}_2 = (1/2)\mathrm{d}|\hat{\mathbf{e}}_2|^2/\mathrm{d}t = 0$ and dividing by $\cos\psi$,[3] yields the differential equation for the angle, $\dot{\psi} = \Omega$, where the time-dependent frequency Ω can be expressed as

$$\Omega = -\hat{\mathbf{e}}_1 \dot{\hat{\mathbf{e}}}_2 + \hat{\mathbf{e}}_2 \cdot (\tilde{\boldsymbol{\omega}} \times \hat{\mathbf{e}}_1) = -\hat{\mathbf{e}}_1 \cdot \dot{\hat{\mathbf{e}}}_2 + \tilde{\boldsymbol{\omega}} \cdot (\hat{\mathbf{e}}_1 \times \hat{\mathbf{e}}_2) = -\hat{\mathbf{e}}_1 \cdot \dot{\hat{\mathbf{e}}}_2 + \tilde{\boldsymbol{\omega}} \cdot \hat{\mathbf{u}}_3 = -\hat{\mathbf{e}}_1 \cdot \dot{\hat{\mathbf{e}}}_2 + \tilde{\boldsymbol{\omega}} \cdot \tilde{\mathbf{L}}/L.$$

It follows from Eq. (3.9) and (3.10) that

$$\hat{\mathbf{e}}_1 \cdot \dot{\hat{\mathbf{e}}}_2 = \frac{\tilde{L}_3(\tilde{L}_2 \dot{\tilde{L}}_1 - \tilde{L}_1 \dot{\tilde{L}}_2)}{L\tilde{L}_{\perp}^2}.$$

Using Eq. (2.17) yields $\dot{\tilde{L}}_1 = \tilde{\omega}_3 \tilde{L}_2 - \tilde{\omega}_2 \tilde{L}_3$ and $\dot{\tilde{L}}_2 = \tilde{\omega}_1 \tilde{L}_3 - \tilde{\omega}_3 \tilde{L}_1$, whence $\Omega = L(\tilde{L}_1 \tilde{\omega}_1 + \tilde{L}_2 \tilde{\omega}_2)/\tilde{L}_{\perp}^2$, or, expressed in terms of conserved quantities and $\tilde{\omega}_3$ only,

$$\Omega = \frac{L(2E_{\mathrm{R}} - I_3 \tilde{\omega}_3^2)}{L^2 - I_3^2 \tilde{\omega}_3^2}. \tag{3.20}$$

The angle ψ is then given by

$$\psi = \int_0^t \mathrm{d}t' \Omega(t'). \tag{3.21}$$

---

[3] When $\cos\psi = 0$, one can instead take the inner product with $\hat{\mathbf{e}}_1$ and divide by $\sin\psi$, with the same result.

The formal result for the matrix **P**, given by Eqs. (3.13)–(3.19), (3.20) and (3.21), still contains a time integral for ψ whose integrand depends on the angular velocity component $\tilde{\omega}_3$. Hence the time dependence of this component of the angular velocity must be specified to perform the integral and obtain ψ. The solution of the components of the angular velocity in the body frame follows from the Euler equations, which can be analyzed in three separate cases depending on the values of the principal moments of inertia.

3.1. Spherical top

For a spherical top, all moments of inertia are the same: $I_1 = I_2 = I_3$, and the Euler equations in Eq. (2.17) become extremely simple, namely, $\dot{\tilde{\omega}}_j = 0$. For the spherical top system, all components of the angular velocity in the body frame are therefore constant, and hence the components of the angular momentum in the body frame are constant as well. It therefore follows that the matrix $\mathbf{T}_1'$ in Eq. (3.13) remains constant in time, so that

$$\mathbf{T}_1 = \mathbf{T}_1'\mathbf{T}_1'^{\dagger}(0) = \mathbf{1}. \tag{3.22}$$

The frequency Ω can also easily be determined by noting that $\tilde{\omega}_3$ is constant and $I_1 = I_2 = I_3$, so that Eq. (3.20) gives

$$\Omega = \frac{L(I_1\tilde{\omega}_1^2 + I_2\tilde{\omega}_2^2)}{I_1^2\tilde{\omega}_1^2 + I_2^2\tilde{\omega}_2^2} = \frac{L}{I_1} = |\boldsymbol{\omega}|, \tag{3.23}$$

leading to $\psi = \Omega t = |\omega|t$. Eq. (3.19) then gives, with $\boldsymbol{L}(0)/L = \boldsymbol{\omega}/\Omega$,

$$\mathbf{T}_2 = \mathbf{U}(-\boldsymbol{\omega}t), \tag{3.24}$$

so that one recovers the well-known result that for a spherical rotor

$$\mathbf{P} = \mathbf{T}_1\mathbf{T}_2 = \mathbf{U}(-\boldsymbol{\omega}t). \tag{3.25}$$

The rotation matrix **P** corresponds to a rotation by an angle of $-|\omega|t$ around the axis $\omega/|\omega|$. Note that the minus sign in the angle arises here from the fact that if the body rotates one way, the lab frame, as seen from the body frame, rotates in the opposite way.

3.2. Symmetric top

For the case of a symmetric top, $I_1 = I_2$ but $I_2 \neq I_3$. In that case, one can solve the Euler equations (2.17) in terms of well-known functions:

$$\begin{aligned}
\tilde{\omega}_1 &= \tilde{\omega}_1(0)\cos\omega_p t + \tilde{\omega}_2(0)\sin\omega_p t, \\
\tilde{\omega}_2 &= -\tilde{\omega}_1(0)\sin\omega_p t + \tilde{\omega}_2(0)\cos\omega_p t, \\
\tilde{\omega}_3 &= \tilde{\omega}_3(0).
\end{aligned} \tag{3.26}$$

Here, the precession frequency ω_p is given by $\omega_p = (1 - I_3/I_1)\tilde{\omega}_3(0)$. From these equations, it is evident that $\tilde{L}_\perp = I_1[\tilde{\omega}_1^2 + \tilde{\omega}_2^2]^{1/2}$ is conserved for a symmetric top, which allows one to rewrite $\mathbf{T}_1$ in Eq. (3.17) as a rotation around the z-axis by an angle of $-\omega_p t$:

$$\mathbf{T}_1 = \begin{pmatrix} \cos\omega_p t & \sin\omega_p t & 0 \\ -\sin\omega_p t & \cos\omega_p t & 0 \\ 0 & 0 & 1 \end{pmatrix} = \mathbf{U}(-\omega_p t\hat{\boldsymbol{z}}). \tag{3.27}$$

The final rotation angle ψ can be determined by noting that

$$\Omega = \frac{L(I_1\tilde{\omega}_1^2 + I_2\tilde{\omega}_2^2)}{I_1^2\tilde{\omega}_1^2 + I_2^2\tilde{\omega}_2^2} = \frac{L}{I_1}. \tag{3.28}$$

Again this is a constant but, in contrast to the spherical case, no longer equal to $|\omega|$, so

$$\psi = \Omega t. \tag{3.29}$$

The second rotation $\mathbf{T}_2$ in Eq. (3.16) is therefore given by Eq. (3.19) with $\psi = Lt/I_1$, i.e.,

$$\mathbf{T}_2 = \mathbf{U}(-\tilde{\boldsymbol{L}}(0)t/I_1). \tag{3.30}$$

As a result, the rotation matrix $\mathbf{P}$ for a symmetric top is given by

$$\mathbf{P} = \mathbf{T}_1\mathbf{T}_2 = \mathbf{U}(-\omega_p t\hat{\boldsymbol{z}})\mathbf{U}(-\tilde{\boldsymbol{L}}(0)t/I_1). \tag{3.31}$$

3.3. Asymmetric top

For a general asymmetric top, all moments of inertia are distinct: $I_1 \neq I_2 \neq I_3 \neq I_1$. The moments of inertia can be ordered in increasing order of magnitude, and we will choose to call the middle one always I_2, while either I_1 or I_3 is the largest one. In the absence of forces and torques, Eq. (2.17) is integrable since the energy E_R and the norm of the angular momentum L are conserved quantities in the body frame. To ensure all quantities occurring in the solutions are real-valued (rather than complex-valued), one needs to consider the quantities E_R and $L^2/(2I_2)$ and make sure that [18]

$$\begin{aligned} I_1 > I_2 > I_3 \quad &\text{if } E_R > \frac{L^2}{2I_2}, \\ I_1 < I_2 < I_3 \quad &\text{if } E_R < \frac{L^2}{2I_2}. \end{aligned} \tag{3.32}$$

We will refer to this as the Jacobi ordering. Either situation can always be realized by choosing which principal axis of the body to call the first, second or third.

Once the Jacobi ordering is adopted, the solution of the Euler equations is given by [18–20]

$$\tilde{\omega}_1 = \tilde{\omega}_{1m}\text{cn}(\omega_p t + \varepsilon|m), \tag{3.33}$$
$$\tilde{\omega}_2 = \tilde{\omega}_{2m}\text{sn}(\omega_p t + \varepsilon|m), \tag{3.34}$$
$$\tilde{\omega}_3 = \tilde{\omega}_{3m}\text{dn}(\omega_p t + \varepsilon|m), \tag{3.35}$$

where sn, cn and dn are Jacobi elliptic functions [21–23], and

$$\tilde{\omega}_{1m} = \text{sgn}(\tilde{\omega}_1(0))\sqrt{\frac{L^2 - 2I_3 E_R}{I_1(I_1 - I_3)}}, \tag{3.36}$$

$$\tilde{\omega}_{2m} = -\text{sgn}(\tilde{\omega}_1(0))\sqrt{\frac{L^2 - 2I_3 E_R}{I_2(I_2 - I_3)}}, \tag{3.37}$$

$$\tilde{\omega}_{3m} = \text{sgn}(\tilde{\omega}_3(0))\sqrt{\frac{L^2 - 2I_1 E_R}{I_3(I_3 - I_1)}}, \tag{3.38}$$

$$\omega_p = \text{sgn}(I_2 - I_3)\text{sgn}(\tilde{\omega}_3(0))\sqrt{\frac{(L^2 - 2I_1 E_R)(I_3 - I_2)}{I_1 I_2 I_3}}, \tag{3.39}$$

$$m = \frac{(L^2 - 2I_3 E_R)(I_1 - I_2)}{(L^2 - 2I_1 E_R)(I_3 - I_2)}, \tag{3.40}$$

$$\varepsilon = -\omega_p t_0 = F(\tilde{\omega}_2(0)/\tilde{\omega}_{2m}|m), \tag{3.41}$$

where in the last equation, F is the incomplete elliptic integral of the first kind [21], defined as[4]

$$F(x|m) = \int_0^x \frac{\mathrm{d}t}{\sqrt{1 - mt^2}\sqrt{1 - t^2}}. \tag{3.42}$$

---

[4] We deviate here from the somewhat more usual notation $F(\alpha|m) = F(x|m)$ where $x = \sin\alpha$.

To give an idea of the behavior of elliptic functions, Fig. 1 shows a plot of the elliptic functions for two values of the elliptic parameter, $m = 0.81$ and $m = 0.998$. It is evident from the plots that the elliptic functions are periodic functions of their first argument, and resemble the sine, cosine and the constant function 1 unless the value of m is close to one. In other words, the elliptic parameter m determines how closely the elliptic functions resemble their trigonometric counterparts. For $m = 0$, the functions cn, sn and dn reduce to cos, sin and 1, respectively. Note that the constant function 1 is reminiscent of the conservation of $\tilde{\omega}_3$ (cf. Eq. (3.26)) in the case of the symmetric top. Indeed, for $I_1 = I_2$, Eq. (3.40) shows that $m = 0$.

Three more numbers can be derived from the elliptic parameter m which play an important role in the properties of elliptic functions. These are the *quarter-period* $K = F(1|m)$, the *complementary quarter-period* $K' = F(1|1 - m)$ and the *nome* $q = \exp(-\pi K'/K)$, which is a parameter that appears in various series expansions of elliptic functions. In fact, the period of the elliptic functions cn and sn is equal to $4K$, while that of dn is $2K$.

Given the solution of the Euler equations in Eqs. (3.34), (3.35), the matrix $\mathbf{T}'_1$ in Eq. (3.13) is completely specified. On the other hand, to solve for the time dependence of $\mathbf{T}'_2$ in Eq. (3.14), the integral in Eq. (3.21) must be performed. Unlike to previous two cases, the integrand Ω of ψ, as given by Eq. (3.20), is not a constant. Despite this complication, the integral can still be performed explicitly using some properties of elliptic functions as we will now show. It will require a bit of complex analysis to integrate Ω over time, so the reader may wish to skip this technical part and move on to the answer in Eq. (3.54) (where the function ϑ_1 is the first Jacobi function [22,21]).
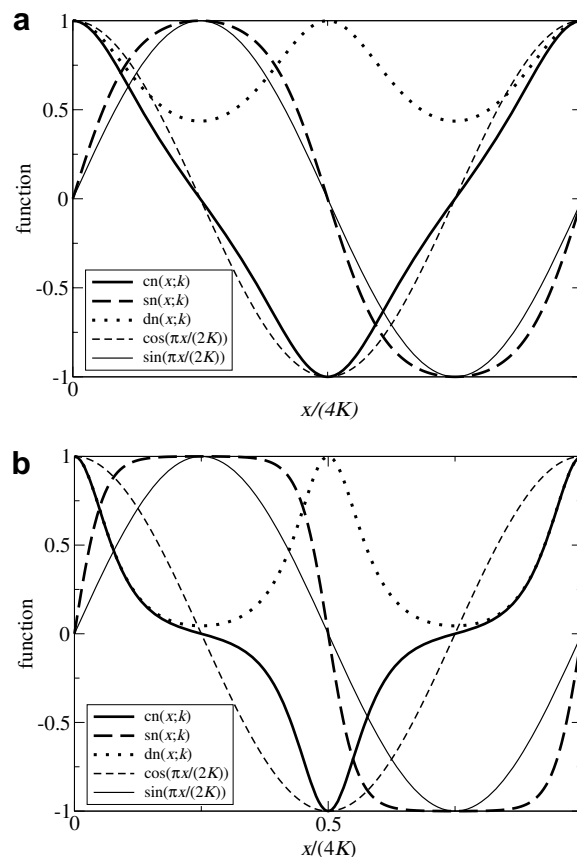

Fig. 1. Examples of the elliptic functions cn (solid line), sn (bold dashed line), dn (dotted line) for (a) $m = 0.81$ ($K = 2.28\ldots$, $q = 0.10\ldots$) and (b) $m = 0.998$ ($K = 4.50\ldots$, $q = 0.33\ldots$). Also plotted are the cosine (short dashed line) and sine (thin short dashed line) with the same period, for comparison.

By definition, an elliptic function is a complex function f (of a complex variable t) that is doubly periodic in the sense that $f(t + \tau) = f(t + \tau') = f(t)$, and whose singularities in the finite complex plane consist only of poles. The doubly periodic function is completely specified by the values it takes inside the *fundamental parallelogram* spanned by τ and τ' in the complex plane. Moreover, it may be shown that an elliptic function is determined by the singularities inside that parallelogram up to an additive constant [22,23]. In fact, for a elliptic function $f(t)$ having n poles of order one at $t = t_{\text{pole}}^{(j)}$ ($j = 1, \ldots, n$) in the fundamental parallelogram with residues r_j, one may write (Ref. [22, §21.5])

$$f(t) = A_2 + \sum_{j=1}^{n} r_j \frac{\mathrm{d}}{\mathrm{d}t} \log \vartheta_1 \left(\frac{\pi(t - t_{\text{pole}}^{(j)})}{\tau} \bigg| m \right), \tag{3.43}$$

where A_2 is an additive constant and $\vartheta_1(u|m)$ is the first Jacobi theta function [22,21].

In order to apply Eq. (3.43), the singularity structure of Ω must be examined. A little analysis shows that the function dn appearing in $\tilde{\omega}_3$ in Eq. (3.35) has only two poles of order one with opposite residues in its fundamental parallelogram, and its periods are $\omega_p \tau = 2K$ and $\omega_p \tau' = 4iK'$ (Ref. [21, §16.2]). Since any rational function of elliptic functions is again an elliptic function, the function Ω in Eq. (3.20) is also an elliptic function with the same periods. From the form of Ω in Eq. (3.20), one easily sees that any pole t_{pole} of Ω in the complex plane is due to a zero of the denominator, i.e.,

$$\tilde{\omega}_3(t_{\text{pole}}) = \pm \frac{L}{I_3}. \tag{3.44}$$

Note that the poles of $\tilde{\omega}_3$ itself cancel in the numerator and the denominator in Eq. (3.20) leading to a limit value of L/I_3, and do not to lead to poles in Ω.

Using Eqs. (3.35), (3.44) is solved by

$$\omega_p t_{\text{pole}} = \pm \mathrm{dn}^{-1} \left(\pm \frac{L}{I_3 \tilde{\omega}_{3m}} \bigg| m \right) - \varepsilon + 2K n_1 + 4K' n_2 i. \tag{3.45}$$

Here n_1 and n_2 are arbitrary integers and the two $\pm$ signs are independent, thus denoting four possibilities. Since dn changes sign when its argument is shifted over a half-period $2K'i$ [21], one $\pm$ sign in Eq. (3.45) can be eliminated by changing the term $+4K'n_2 i$ to $+2K'n_2 i$:

$$\omega_p t_{\text{pole}} = \pm \mathrm{dn}^{-1} \left(\frac{L}{I_3 \tilde{\omega}_{3m}} \bigg| m \right) - \varepsilon + 2K n_1 + 2K' n_2 i.$$

Using that

$$\mathrm{dn}^{-1}(x|m) = \mathrm{i}[K' - F(x^{-1}|1 - m)],$$

(obtained by combining §16.3.3, §16.20.3 and §17.4.46 in Ref. [21]), one finds

$$\omega_p t_{\text{pole}} = \pm \mathrm{i} \left[K' - F\left(\frac{I_3 \tilde{\omega}_{3m}}{L} \bigg| 1 - m \right) \right] - \varepsilon + 2K n_1 + 2K' n_2 i.$$

Noting that for negative values of $\tilde{\omega}_{3m}$, one can write $K' - F(I_3 \tilde{\omega}_{3m}/L|1 - m) = \mathrm{sgn}(\tilde{\omega}_{3m})K' - F(I_3 \tilde{\omega}_{3m}/L|1 - m) + 2K'$, we can rewrite this as

$$\omega_p t_{\text{pole}} = \pm \mathrm{i}\eta - \varepsilon + 2K n_1 + 2K' n_2 i, \tag{3.46}$$

where we have defined

$$\eta = \mathrm{sgn}(\tilde{\omega}_{3m})K' - F\left(\frac{I_3 \tilde{\omega}_{3m}}{L} \bigg| 1 - m \right). \tag{3.47}$$

Note that $-K' \leqslant \eta \leqslant K'$.

The periodic structure in Eq. (3.46) can be understood as follows. The function Ω depends on t though dn^2, and dn has periods $2K$ and $4K'i$. Note that even though dn changes sign when its argument is shifted over $2K'i$, this sign change leaves dn^2 and hence Ω unchanged. From these considerations, it is evident that the actual

periods of Ω are $2K/\omega_p$ and $2K'i/\omega_p$. Although the size of the fundamental parallelogram is dictated by the function under consideration, the choice of its origin is free. Choosing the fundamental parallelogram to be $([-K - K'i]/\omega_p, [-K + K'i]/\omega_p)$, the two poles in the parallelogram are complex conjugates t_{pole} and t^*_{pole}, where

$$\omega_p t_{\text{pole}} = -\varepsilon + i\eta. \tag{3.48}$$

The pole structure of the function $\Omega(t)$ is illustrated in Fig. 2.

It is straightforward to show that the residues of Ω at these poles are given by $r = \frac{i}{2}$ for the pole at t_{pole} and $-r = -\frac{i}{2}$ for the pole at t^*_{pole}, so that, using Eq. (3.43) with $\tau = 2K/\omega_p$, the integrand Ω may be written as

$$\Omega = A_2 + \frac{i}{2}\frac{d}{dt}\left[\log \vartheta_1\left(\frac{\pi}{2K}(\omega_p t + \varepsilon - i\eta)\Big|m\right) - \log \vartheta_1\left(\frac{\pi}{2K}(\omega_p t + \varepsilon + i\eta)\Big|m\right)\right], \tag{3.49}$$

and further manipulated to obtain a form that can be easily integrated,

$$\Omega = A_2 + \frac{i}{2}\frac{d}{dt}\left[\log \vartheta_1\left(\frac{\pi}{2K}(\omega_p t + \varepsilon - i\eta)\Big|m\right) - \left\{\log \vartheta_1\left(\frac{\pi}{2K}(\omega_p t + \varepsilon - i\eta)\Big|m\right)\right\}^*\right]$$

$$= A_2 - \frac{d}{dt}\text{Im}\log \vartheta_1\left(\frac{\pi}{2K}(\omega_p t + \varepsilon - i\eta)\Big|m\right) = A_2 - \frac{d}{dt}\arg\vartheta_1\left(\frac{\pi}{2K}(\omega_p t + \varepsilon - i\eta)\Big|m\right). \tag{3.50}$$

The constant A_2 appearing in Eq. (3.50) can be obtained using the point $t = t_0 = -\varepsilon/\omega_p$, at which time $\tilde{\omega}_2 = 0$ (cf. Eq. (3.34)) and Eq. (3.20) gives

$$\Omega(t_0) = \frac{L}{I_1}. \tag{3.51}$$

Examining the right hand side of Eq. (3.50), noting that

$$\frac{d}{dt}\log \vartheta_1\left(\frac{\pi}{2K}(\omega_p t + \varepsilon - i\eta)\Big|m\right) = \frac{\pi\omega_p}{2K}\frac{d}{du}\log \vartheta_1\left(u = \frac{\pi}{2K}(\omega_p t + \varepsilon - i\eta)\Big|m\right)$$

$$= \frac{\pi\omega_p}{2K}\frac{\vartheta_1'\left(\frac{\pi}{2K}(\omega_p t + \varepsilon - i\eta)\big|m\right)}{\vartheta_1\left(\frac{\pi}{2K}(\omega_p t + \varepsilon - i\eta)\big|m\right)},$$

and using $\vartheta_1(-u|m) = -\vartheta_1(u|m)$, Eq. (3.49) gives

$$\Omega(t_0) = A_2 - \frac{\pi\omega_p}{2K}\frac{\vartheta_1'\left(\frac{i\pi\eta}{2K}\big|m\right)}{\vartheta_1\left(\frac{i\pi\eta}{2K}\big|m\right)}. \tag{3.52}$$

Comparing Eqs. (3.51) and (3.52), we see that

$$A_2 = \frac{L}{I_1} + i\frac{\pi\omega_p}{2K}\frac{\vartheta_1'\left(\frac{i\pi\eta}{2K}\big|m\right)}{\vartheta_1\left(\frac{i\pi\eta}{2K}\big|m\right)}. \tag{3.53}$$
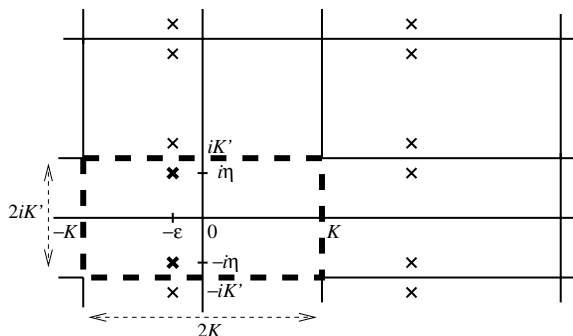

Fig. 2. Periodic pole structure in the complex plane of the function $\Omega(t)$ as a function of the variable $u = \omega_p t$. The fundamental parallelogram is indicated by a bold dashed rectangle and the crosses are poles.

Eq. (3.50) is now readily integrated to express the angle ψ in terms of the theta function as:

$$\psi = \int_0^t \mathrm{d}t' \Omega(t') = A_1 + A_2 t - \arg \vartheta_1 \left(\frac{\pi}{2K} (\omega_p t + \varepsilon - \mathrm{i}\eta) \Big| m \right), \tag{3.54}$$

where

$$A_1 = \arg \vartheta_1 \left(\frac{\pi(\varepsilon - \mathrm{i}\eta)}{2K} \Big| m \right), \tag{3.55}$$

and A_2 is given by Eq. (3.53).

With this expression for ψ, the matrix $\mathbf{P} = \mathbf{T}_1' \mathbf{T}_2' \mathbf{T}_1'^{\dagger}(0)$ is now fully specified, with $\mathbf{T}_1$ and $\mathbf{T}_2$ given in Eqs. (3.13) and (3.14), respectively. Unlike the special cases of spherical and symmetric rotors, no further simplifications occur in the expressions for these matrices.

4. Numerical issues

In this section an efficient implementation of computing the exact solutions presented in the previous section is outlined. Because the rotation matrices for spherical and symmetric tops in Eqs. (3.25) and (3.31) are easily implemented using Rodrigues' formula [16], we focus on the case of an asymmetric rigid rotor. For this case, the attitude matrix was expressed in terms of complex theta functions, which hinders a straightforward and efficient numerical implementation. First it will be shown how all matrix elements in the attitude matrix may expressed in terms of real quantities and implemented efficiently. At the end of the section, an algorithm to compute the motion of an asymmetric rigid body will be presented.

4.1. Implementation

As discussed above, the matrix $\mathbf{P}$ can generally be written as a product of two rotation matrices in the form $\mathbf{T}_1 \mathbf{T}_2$, or three rotations in the form $\mathbf{T}_1' \mathbf{T}_2' \mathbf{T}_1'^{\dagger}(0)$. For the implementation of the free motion of the asymmetric top, we prefer the latter because it does not require Rodrigues' formula to be applied twice and the matrix $\mathbf{T}_2'$ is sparse which allows an efficient matrix multiplication. The extra matrix multiplication with $\mathbf{T}_1'^{\dagger}(0)$ can be circumvented by using $\mathbf{B} = \mathbf{T}_1'^{\dagger}(0)\mathbf{A}(0)$. The matrix $\mathbf{T}_1'$ is given in Eq. (3.13) in terms of the components of the angular momentum in the body frame, $\tilde{L}_j = I_j \tilde{\omega}_j$. The $\tilde{\omega}_j$ are given by Eqs. (3.33)–(3.35), which involve the elliptic functions.

Although the occurrence of elliptic functions may seem complicated, there are standard numerical methods to calculate the elliptic functions sn, cn and dn [21,24,25] that are very efficient and which makes them no more problematic to use than standard transcendental functions such as sin or cos. The matrix $\mathbf{T}_1'$ can therefore be computed numerically in a straightforward way in terms of the standard elliptic functions.

The matrix $\mathbf{T}_2'$ is given in Eq. (3.14) and is a rotation by an angle ψ around the z-axis, with ψ given in (3.54). As is evident from Eq. (3.14), only $\sin\psi$ and $\cos\psi$ rather than the angle ψ itself need to be evaluated to construct $\mathbf{T}_2'$. Using Eq. (3.54) and the addition formulas for cos and sin, these may be expressed as

$$\begin{aligned}
\cos\psi &= \cos(A_1 + A_2 t) \cos \arg \vartheta_1 + \sin(A_1 + A_2 t) \sin \arg \vartheta_1 \\
&= \frac{\cos(A_1 + A_2 t) \operatorname{Re} \vartheta_1 + \sin(A_1 + A_2 t) \operatorname{Im} \vartheta_1}{\sqrt{(\operatorname{Re} \vartheta_1)^2 + (\operatorname{Im} \vartheta_1)^2}},
\end{aligned} \tag{4.1}$$

$$\begin{aligned}
\sin\psi &= \sin(A_1 + A_2 t) \cos \arg u - \cos(A_1 + A_2 t) \sin \arg u \\
&= \frac{\sin(A_1 + A_2 t) \operatorname{Re} \vartheta_1 - \cos(A_1 + A_2 t) \operatorname{Im} \vartheta_1}{\sqrt{(\operatorname{Re} \vartheta_1)^2 + (\operatorname{Im} \vartheta_1)^2}}.
\end{aligned} \tag{4.2}$$

where $\vartheta_1 = \vartheta_1 \left(\frac{\pi}{2K} (\omega_p t + \varepsilon - \mathrm{i}\eta) | m \right)$. Clearly, to compute these expressions, the real and imaginary parts of ϑ_1 as well as the real constants A_1 and A_2 must be computed.

Noting that the function ϑ_1 has the following series expansion in the nome q (Ref. [21, §16.27.1]),

$$\vartheta_1(u|m) = 2q^{1/4} \sum_{n=0}^{\infty} (-1)^n q^{n(n+1)} \sin[(2n+1)u], \tag{4.3}$$

the real and imaginary parts of ϑ_1 in Eq. (4.3) for a complex argument $u = \frac{\pi}{2K}(\omega_p t + \varepsilon - i\eta)$, can be written as

$$\operatorname{Re}\vartheta_1 = 2q^{1/4} \sum_{n=0}^{\infty} (-1)^n q^{n(n+1)} \cosh\frac{(2n+1)\pi\eta}{2K} \sin\frac{(2n+1)\pi(\omega_p t + \varepsilon)}{2K},$$

$$\operatorname{Im}\vartheta_1 = -2q^{1/4} \sum_{n=0}^{\infty} (-1)^n q^{n(n+1)} \sinh\frac{(2n+1)\pi\eta}{2K} \cos\frac{(2n+1)\pi(\omega_p t + \varepsilon)}{2K}. \tag{4.4}$$

The convergence of these series is extremely rapid due to the appearance of the $q^{n(n+1)}$. In practice one rarely needs more than three or four terms to get to machine precision.

Based on the series expansion of ϑ_1, the constant A_1 given in Eq. (3.55) can be evaluated as follows:

$$A_1 = n\pi + \arctan\frac{\operatorname{Im}\vartheta_1\left(\frac{\pi}{2K}(\varepsilon - i\eta)|m\right)}{\operatorname{Re}\vartheta_1\left(\frac{\pi}{2K}(\varepsilon - i\eta)|m\right)}, \tag{4.5}$$

where $n = 0$ if $\operatorname{Re}\vartheta_1 > 0$, $n = 1$ if $\operatorname{Re}\vartheta_1 < 0$ and $\operatorname{Im}\vartheta > 0$, and $n = -1$ if $\operatorname{Re}\vartheta_1 < 0$ and $\operatorname{Im}\vartheta_1 < 0$.

For the constant A_2, an expansion of the logarithmic derivative of ϑ_1 can be utilized (Ref. [21, §16.29.1]):

$$\frac{\vartheta_1'(u|m)}{\vartheta_1(u|m)} = \cot u + 4\sum_{n=1}^{\infty} \frac{q^{2n}}{1-q^{2n}} \sin 2nu. \tag{4.6}$$

Using the expression for A_2 in Eq. (3.53), where $u = i\pi\eta/(2K)$ is purely imaginary and noting that $\cot i\, u = -i\coth u = (e^{2u}-1)/(e^{2u}+1)$ and $\sin iu = i\sinh u = (e^u - e^{-u})/2$, one can write

$$i\frac{\vartheta_1'(iu|m)}{\vartheta_1(iu|m)} = \frac{e^{2u}+1}{e^{2u}-1} - 2\sum_{n=1}^{\infty} \frac{q^{2n}}{1-q^{2n}}(e^{2nu} - e^{-2nu}). \tag{4.7}$$

Using the series expansion in Eq. (4.7), A_2 can be evaluated from

$$A_2 = \frac{L}{I_1} + \frac{\pi\omega_p}{2K}\left[\frac{\xi+1}{\xi-1} - 2\sum_{n=1}^{\infty}\frac{q^{2n}}{1-q^{2n}}(\xi^n - \xi^{-n})\right], \tag{4.8}$$

where

$$\xi = e^{\pi\eta/K}. \tag{4.9}$$

The series in Eq. (4.8) converges if $\xi q^2 < 1$. Because $-K < \eta < K'$ and $q = \exp(-\pi K'/K)$, one has $\xi q^2 < q < 1$ so this series converges, and, because q is typically small, usually quickly.

The above derivation assumed that the Jacobi ordering of Eq. (3.32) was satisfied. Although this can always be realized by choosing which principal axis of the body to call the first, second or third, as is evident from Eq. (3.32), the choice of principal axes depends on the initial values of the angular velocities. Often, instead of choosing the axis depending on the initial conditions, it is preferable to work with a fixed convention in which the principal axes are oriented in a particular way with respect to the masses of the body. In that case, one can adopt the Jacobi ordering convention by introducing internal variables which differ when necessary from the physical ones by a rotation. For instance, if $I_1 > I_2 > I_3$ but it should be $I_1 < I_2 < I_3$ according to Eq. (3.32), one can apply the rotation matrix

$$\mathbf{U}^* \equiv \begin{pmatrix} 0 & 0 & 1 \\ 0 & -1 & 0 \\ 1 & 0 & 0 \end{pmatrix}, \tag{4.10}$$

which transforms between the internal and physical choices of principal axes by exchanging the x and z components and reversing the y component. If the order of the moments of inertia already follows the Jacobi ordering, $\mathbf{U}^*$ is effectively the identity matrix.

4.2. Algorithm for the asymmetric top

Based on the above, the following algorithm can be set up to calculate the position of a rigid body at any arbitrary time, given a set of initial conditions. For efficiency, the algorithm consists of two steps: an initialization routine, in which some expressions are pre-calculated, and an evolution routine that calculates $\tilde{\boldsymbol{\omega}}$ and $\mathbf{A}$ at time t.

In the algorithm below, the functions sn, cn, dn and F are assumed to be available, but not the ϑ_1 function. See Refs. [24,25] for implementations of sn, cn, dn and F.

The initialization routine takes an initial angular velocity vector in the body frame $\tilde{\boldsymbol{\omega}}(0) = (\omega_{x0}, \omega_{y0}, \omega_{z0})$ and inertial moments I_x, I_y and I_z (where it is assumed that I_y is the middle one), and pre-computes a few variables as follows (in pseudo-code, in order to facilitate implementations in different programming languages):

```
Initialization(I_x, I_y, I_z, ω̃_x0, ω̃_y0, ω̃_z0, A(0))
   COMPUTE L² = I_x²ω̃_x0² + I_y²ω̃_y0² + I_z²ω̃_z0²
   COMPUTE 2E = I_xω̃_x0² + I_yω̃_y0² + I_zω̃_z0²
   IF (2E > L²/I_y AND I_x < I_z) OR (2E < L²/I_y AND I_x > I_z) THEN
      SET orderflag
      SET I_1 = I_z, I_2 = I_y and I_3 = I_x
      SET ω_10 = ω_z0, ω_20 = -ω_y0 and ω_30 = ω_x0
      COMPUTE L_⊥ = √(I_1²ω_10² + I_2²ω_20²)
```

$$\text{COMPUTE } [\mathbf{T}_1'^{\dagger}(0)\mathbf{U}^*] = \begin{pmatrix} -\frac{L_\perp}{L} & -\frac{I_2 I_3 \omega_{20}\omega_{30}}{LL_\perp} & \frac{I_1 I_3 \omega_{10}\omega_{30}}{LL_\perp} \\ 0 & -\frac{I_1\omega_{10}}{L_\perp} & -\frac{I_2\omega_{20}}{L_\perp} \\ \frac{I_3\omega_{30}}{L} & -\frac{I_2\omega_{20}}{L} & \frac{I_1\omega_{10}}{L} \end{pmatrix}$$

```
   ELSE
      UNSET orderflag
      SET I_1 = I_x, I_2 = I_y and I_3 = I_z
      SET ω_10 = ω_x0, ω_20 = ω_y0 and ω_30 = ω_z0
      COMPUTE L_⊥ = √(I_1²ω_10² + I_2²ω_20²)
```

$$\text{COMPUTE } [\mathbf{T}_1'^{\dagger}(0)\mathbf{U}^*] = \begin{pmatrix} \frac{I_1 I_3 \omega_{10}\omega_{30}}{LL_\perp} & \frac{I_2 I_3 \omega_{20}\omega_{30}}{LL_\perp} & -\frac{L_\perp}{L} \\ -\frac{I_2\omega_{20}}{L_\perp} & \frac{I_1\omega_{10}}{L_\perp} & 0 \\ \frac{I_1\omega_{10}}{L} & \frac{I_2\omega_{20}}{L} & \frac{I_3\omega_{30}}{L} \end{pmatrix}$$

```
   END IF
   COMPUTE B = [T_1'†(0)U*]A(0)
   COMPUTE ω_1m = sgn(ω_10)√((L² - 2EI_3)/(I_1(I_1 - I_3)))
   COMPUTE ω_2m = -sgn(ω_10)√((L² - 2EI_3)/(I_2(I_2 - I_3)))
   COMPUTE ω_3m = sgn(ω_30)√((L² - 2EI_1)/(I_3(I_3 - I_1)))
   COMPUTE ω_p = sgn(I_2 - I_3)sgn(ω_30)√((L² - 2EI_1)(I_3 - I_2)/(I_1 I_2 I_3))
   COMPUTE m = (L² - 2EI_3)(I_1 - I_2)/((L² - 2EI_1)(I_3 - I_2))
   COMPUTE ε = F(ω_20/ω_2m|m)
   COMPUTE K = F(1|m)
   COMPUTE K' = F(1|1 - m)
   COMPUTE q = exp(-πK'/K)
   COMPUTE η = sgn(ω_30)K' - F(I_3ω_3m/L, 1 - m)
   COMPUTE ξ = exp(πη/K)
   SET A_2 = L/I_1 + πω_p(ξ + 1)/(2K(ξ - 1))
   SET n = 1
   REPEAT
```

```
        COMPUTE δA₂ = −(πωₚ/K)(q²ⁿ/(1 − q²ⁿ))(ξⁿ − ξ⁻ⁿ)
        INCREMENT A₂ by δA₂
        INCREMENT n by 1
     UNTIL δA₂ < machine precision
     COMPUTE NT = log(machine precision)/log q
     SET r₀ = 0 and i₀ = 0
     FOR n = 0 TO NT DO
        COMPUTE cᵣ[n] = (−1)ⁿ2qⁿ⁽ⁿ⁺¹⁾⁺¹ᐟ⁴ cosh (2n+1)πη/2K

        COMPUTE cᵢ[n] = (−1)ⁿ⁺¹2qⁿ⁽ⁿ⁺¹⁾⁺¹ᐟ⁴ sinh (2n+1)πη/2K
        INCREMENT r₀ by cᵣ[n] sin (2n+1)πε/2K
        INCREMENT i₀ by cᵢ[n] cos (2n+1)πε/2K
     END FOR
     IF r₀ > 0 THEN k = 0 ELSE k = sgn(i₀)
     COMPUTE A₁ = arctan(i₀/r₀) + kπ
     STORE orderflag, I₁, I₂, I₃, ω₁ₘ, ω₂ₘ, ω₃ₘ, m, ωₚ, ε, A₁, A₂, NT, cᵣ[], cᵢ[] and B
  END Initialization
```

The evolution routine can use the pre-computed expressions in the following way:

```
  Evolution (t)
     COMPUTE ω̃₁ = ω₁ₘcn(ωₚt + ε|m)
     COMPUTE ω̃₂ = ω₂ₘsn(ωₚt + ε|m)
     COMPUTE ω̃₃ = ω₃ₘdn(ωₚt + ε|m)
     SET Re ϑ₁ = 0 and Im ϑ₁ = 0
     FOR n = 0 TO NT DO
        INCREMENT Re ϑ₁ by cᵣ[n]sin((2n + 1)π(ωₚt + ε)/(2K))
        INCREMENT Im ϑ₁ by cᵢ[n]cos((2n + 1)π(ωₚt + ε)/(2K))
     END FOR
     COMPUTE C = cos(A₁ + A₂t), S = sin(A₁ + A₂t)
```

$$\text{COMPUTE } \cos\psi = (C\,\mathrm{Re}\,\vartheta_1 + S\,\mathrm{Im}\,\vartheta_1)/\sqrt{\mathrm{Re}\,\vartheta_1^2 + \mathrm{Im}\,\vartheta_1^2}$$

$$\text{COMPUTE } \sin\psi = (S\,\mathrm{Re}\,\vartheta_1 - C\,\mathrm{Im}\,\vartheta_1)/\sqrt{\mathrm{Re}\,\vartheta_1^2 + \mathrm{Im}\,\vartheta_1^2}$$

$$\text{COMPUTE } L_\perp = \sqrt{I_1^2\omega_1^2 + I_2^2\omega_2^2}$$

```
     IF orderflag IS SET THEN
        COMPUTE
```

$$[\mathbf{U}^*\mathbf{T}_1'] = \begin{pmatrix} -\frac{L_\perp}{L} & 0 & \frac{I_3\omega_3}{L} \\ -\frac{I_2 I_3 \tilde{\omega}_2 \tilde{\omega}_3}{L L_\perp} & -\frac{I_1 \tilde{\omega}_1}{L_\perp} & -\frac{I_2 \tilde{\omega}_2}{L} \\ \frac{I_1 I_3 \tilde{\omega}_1 \tilde{\omega}_3}{L L_\perp} & -\frac{I_2 \tilde{\omega}_2}{L_\perp} & \frac{I_1 \tilde{\omega}_1}{L} \end{pmatrix}$$

```
        SWAP ω̃₁ and ω̃₃
        CHANGE SIGN of ω̃₂
     ELSE
        COMPUTE
```

$$[\mathbf{U}^*\mathbf{T}_1'] = \begin{pmatrix} \frac{I_1 I_3 \tilde{\omega}_1 \tilde{\omega}_3}{L L_\perp} & -\frac{I_2 \tilde{\omega}_2}{L_\perp} & \frac{I_1 \tilde{\omega}_1}{L} \\ \frac{I_2 I_3 \tilde{\omega}_2 \tilde{\omega}_3}{L L_\perp} & \frac{I_1 \tilde{\omega}_1}{L_\perp} & \frac{I_2 \tilde{\omega}_2}{L} \\ -\frac{L_\perp}{L} & 0 & \frac{I_3\omega_3}{L} \end{pmatrix}$$

```
    END IF
    COMPUTE
```

$$\mathbf{A} = [\mathbf{U}^*\mathbf{T}_1'] \begin{pmatrix} \cos\psi & \sin\psi & 0 \\ -\sin\psi & \cos\psi & 0 \\ 0 & 0 & 1 \end{pmatrix} \mathbf{B}$$

```
    RETURN ω̃₁, ω̃₂, ω̃₃ and A
  END Evolution
```

Some remarks about this pseudo-code:

- The `orderflag` indicates whether the Jacobi ordering convention Eq. (3.32) is satisfied. If not, $\mathbf{U}^*$ in Eq. (4.10) is used. If Eq. (3.32) is satisfied, $\mathbf{U}^*$ is set equal to the identity matrix.
- With these definitions, $\mathbf{P}$ is replaced by $\mathbf{U}^*\mathbf{P}\mathbf{U}^*$. This is accomplished simply by $\mathbf{T}_1' \rightarrow \mathbf{U}^*\mathbf{T}_1'$.
- As a consequence, $\mathbf{U}^*$ in Eq. (4.10) is only implicitly used in the combination $[\mathbf{U}^*\mathbf{T}_1']$
- The initial value of $\mathbf{A}(0)$ occurs as $\mathbf{A}(t) = \mathbf{U}^*\mathbf{T}_1'\mathbf{T}_2'\mathbf{T}_1'^\dagger(0)\mathbf{U}^*\mathbf{A}(0)$, so in the initialization routine, we only need to store the combination $\mathbf{B} = \mathbf{T}_1'^\dagger(0)\mathbf{U}^*\mathbf{A}(0)$.
- The `machine precision` depends on the floating point precision used in the calculation; for 64 bit double precision, this is of the order of 10^{-15} to 10^{-16}.
- For clarity of the algorithm, matrix products have not been explicitly written out, and efficiency improvements such as computing intermediate expressions and using a recursive evaluation for the sin's and cos's have not been shown here.
- An implementation of this code in C, which includes these improvements, can be found on the internet at http://www.chem.utoronto.ca/staff/JMS/rigidrotor.html.

5. Example

As an example, consider an object composed of six point masses which are arranged, in the body frame, at the points $(a,0,0)$, $(-a,0,0)$, $(0,b,0)$, $(0,-b,0)$, $(0,0,c)$ and $(0,0,-c)$. All points are assumed to have unit mass, so that the inertial moments are given by $I_1 = 2(b^2 + c^2)$, $I_2 = 2(a^2 + c^2)$ and $I_3 = 2(a^2 + b^2)$. Choosing $a > b > c$ ensures $I_1 < I_2 < I_3$.

In particular we will consider $a = 3$, $b = 2$ and $c = 1$, yielding $I_1 = 10$, $I_2 = 20$ and $I_3 = 26$. As initial conditions we will take $\mathbf{A}(0) = \mathbf{1}$ and $\omega(0) = (1, 15, 1)$. Because of the large value of the y-component of the angular velocity, one may expect motion to consist primarily of rotation around the y-axis. In Fig. 3a the components of the angular velocity in the body frame have been plotted as a function of time, while in Fig. 3b the projection on the x–z plane of the point masses that in the body frame are located at $(a,0,0)$ (the 'long axis'), $(0,b,0)$ (the 'middle' axis') and $(0,0,c)$ (the 'short axis') are plotted. It is clear that the rotational motion does not consist of small perturbations to a rotation around the y-axis. We stress once more that, up to machine precision, the results in Fig. 3 are exact.

6. Discussion

In this paper, the general solution of the rotational motion of a rigid body in the absence of external torques and forces was derived. Explicit expressions for the angular velocities and the attitude matrix were obtained in terms of real quantities to facilitate numerical evaluation. Note that even though the solution of rotational motion for bodies without a simple mass distribution contains generalizations of the familiar sine and cosine functions, the motion typically appears quite complex and notably different from that of a spherical top.

The general solution of the equations governing rigid body dynamics in the absence of forces and torques presented here is potentially useful in several important applications. The primary advantage of having in hand analytical solutions of the equations of motion of a system lies in the fact that all relevant properties
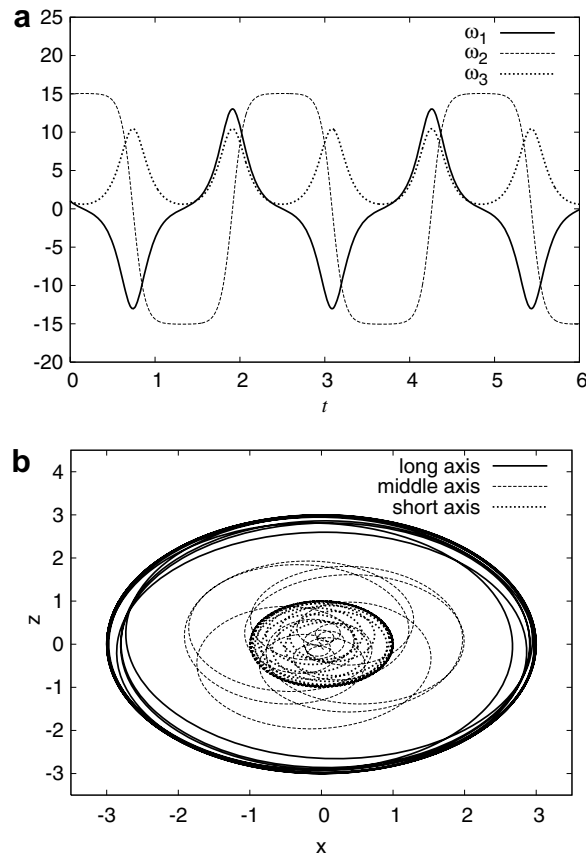
Fig. 3. Example of the exact solution. (a) $\tilde{\omega}(t)$, (b) position of the 'axes'. For details see text.

of a soluble system can be determined at arbitrarily many and arbitrarily distant moments in time. Applications in which knowing exactly the position and orientation of a body at specific moments in time is paramount may benefit from the results presented here. Such applications are abundant in a wide variety of contexts. For example, in astrophysics, many objects such as space crafts, asteroids, certain planets and moons, behave on short time scales as rigid bodies. These bodies are not free since they feel typically weak gravitational fields. However, if their dimensions are small enough compared to the gradients of the gravitational field, gravitational forces effectively influence motion only of the center of mass, while the rotational motion is that of a free rotor described here.

Another obvious application of the solution detailed in this paper is as a diagnostic tool for numerical integration techniques designed for rotating bodies with external torques. Such techniques are of considerable interest, but to establish their accuracy, one needs to be able to compare results of approximate integration schemes with exact results. To date most comparisons are carried out for free systems with a high degree of symmetry and simple rotational motion [10]. Given the relative complexity of motion in the asymmetric case compared with that of a spherical rotor, such comparisons do not appear to be very stringent.

The exact solution is also of practical use in symplectic integrators for use in continuous molecular dynamics [15]. There are already various symplectic integrators using the exact solution of some part of the dynamics [12–14], which generally seems to improve stability and accuracy over simple splitting methods [9–11,26]. However, these do not use the exact solution of the attitude matrix. The integrator of Celledoni and Säfström, for example, uses the exact solution of the Euler equations but uses an approximate expression for the attitude matrix [12]. Using the exact solution of the attitude matrix further improves the stability and accuracy of this integrator [15].

Perhaps the most direct application of the implementation of the exact solution is in simulating complex rigid molecular systems using discontinuous molecular dynamics methods. In this approach, various components of the system interact via discontinuous potentials, leading to impulsive forces and torques that act on molecules at specific moments in time [1,2,27,5,28]. As a result, the motion of all bodies in the system is free between impulsive events that alter the trajectory of the body via discontinuous jumps in the momenta or angular velocities at discrete "collision" times. In order to determine the time at which molecules in the simulation interact, the exact location and orientation of all bodies in the system must be computable at arbitrary times. If the configurations of the system are computed through numerical integration (using e.g. one of the integrators in Refs. [9–12]), such simulations would become inefficient. For this reason, to date, most simulations of rigid bodies interacting via discontinuous potentials have been restricted to systems in which rotational motion is governed by the equations of a spherical rotor (see Refs. [2]). Armed with the results of this paper, the technique of discontinuous molecular dynamics can now be applied to any rigid model—symmetric or asymmetric—with discontinuous interactions of step-potential form. Examples of such studies can be found in Refs. [4].

Acknowledgements

References

[1] B.J. Alder, T.E. Wainwright, Phase transition for a hard sphere system, J. Chem. Phys. 27 (1957) 1208;
B.J. Alder, T.E. Wainwright, Studies in molecular dynamics. I. General method, J. Chem. Phys. 31 (1959) 459;
B.J. Alder, T.E. Wainwright, Studies in molecular dynamics. II. Behavior of a small number of elastic spheres, J. Chem. Phys. 33 (1960) 1439.
[2] G.A. Chapela, S.E. Martínez-Casas, J. Alejandre, Molecular dynamics for discontinuous potentials I. General method and simulation of hard polyatomic molecules, Mol. Phys. 53 (1984) 139;
G.A. Chapela, H.T. Davis, L.E. Sciven, Molecular dynamics of discontinuous Lennard-Jonesium and water, Chem. Phys. 129 (1989) 201;
B.D. Lubachevsky, How to simulate billiards and similar systems, J. Comput. Phys. 94 (1991) 255;
M. Marin, D. Risso, P. Cordero, Efficient algorithms for many-body particle molecular dynamics, J. Comput. Phys. 109 (1993) 306;
A. Donev, S. Torquato, F.H. Stillinger, Neighbor list collision-driven molecular dynamics simulation for nonspherical hard particles. I Algorithmic details, J. Comput. Phys. 202 (2005) 737;
A. Donev, S. Torquato, F.H. Stillinger, Neighbor list collision-driven molecular dynamics simulation for nonspherical hard particles. II Applications to ellipses and ellipsoids, J. Comput. Phys. 202 (2005) 765;
C. De Michele, S. Gabrielli, P. Tartaglia, F. Sciortino, Dynamics in the presence of attractive patchy interactions, J. Phys. Chem. B 110 (2006) 8064.
[3] L. Hernández de la Peña, R. van Zon, J. Schofield, S.B. Opps, Discontinuous molecular dynamics for semi-flexible and rigid bodies. cond-mat/0607527.
[4] L. Hernández de la Peña, R. van Zon, J. Schofield, S.B. Opps, Discontinuous molecular dynamics for rigid bodies: applications. cond-mat/0607528;
L. Hernández de la Peña, R. van Zon, J. Schofield, S.B. Opps, Discontinuous molecular dynamics simulations of water, in preparation.
[5] D. Frenkel, J.F. Maguire, Molecular dynamics study of the dynamical property of an assembly of infinitely thin hard rods, Mol. Phys. 49 (1983) 503;
M.P. Allen, D. Frenkel, J. Talbot, Molecular dynamics simulation using hard particles, Comput. Phys. Rep. 9 (1989) 301;
W. van Ketel, C. Das, D. Frenkel, Structural arrest in an ideal gas, Phys. Rev. Lett. 94 (2005) 135703.
[6] D. Baraff, Dynamic simulation of non-penetrating rigid bodies, Ph.D. thesis, Cornell University, 1992;
D. Baraff, Analytical methods for dynamic simulation of non-penetrating rigid bodies, Comput. Graphics 23 (1989) 223.
[7] J.R. Wertz, Attitude dynamics, in: J.R. Wertz (Ed.), Spacecraft Attitude Determination and Control, Kluwer, Dordrecht, The Netherlands, 1978, pp. 523–528.
[8] Y. Masutani, T. Iwatsu, F. Miyazaki, Motion estimation of unknown rigid body under no external forces and moments, Proc. IEEE Int. Conf. on Robotics and Automation'94, vol. 2, IEEE Computer Society Press, 1994, pp. 1066–1072.
[9] S. Reich, Symplectic integrators for systems of rigid bodies, Fields Inst. Comm. 10 (1996) 181.

[10] A. Dullweber, B. Leimkuhler, R. McLachlan, Symplectic splitting methods for rigid body molecular dynamics, J. Chem. Phys. 107 (1997) 5840.
[11] S.R. Buss, Accurate and efficient simulations of rigid body rotations, J. Comput. Phys. 164 (2000) 377;
T.F. Miller III, M. Eleftheriou, P. Pattnaik, A. Ndirango, D. Newns, G.J. Martyna, Symplectic quaternion scheme for biophysical molecular dynamics, J. Chem. Phys. 116 (2002) 8649;
H. Kamberaj, R.J. Low, M.P. Neal, Time reversible and symplectic integrators for molecular dynamics simulations of rigid molecules, J. Chem. Phys. 122 (2005) 224114.
[12] E. Celledoni, N. Säfström, Efficient time-symmetric simulation of torqued rigid bodies using Jacobi elliptic functions, J. Phys. A, Math. Gen. 39 (2006) 5463.
[13] See appendix C of Ref. [10].
[14] D. Janezic, F. Merzel, An efficient symplectic integration algorithm for molecular dynamics simulations, J. Chem. Inf. Comput. Sci. 35 (1995) 321;
D. Janezic, M. Praprotnik, F. Merzel, Molecular dynamics integration and molecular vibrational theory. I. New symplectic integrators, J. Chem. Phys. 122 (2005) 174101.
[15] R. van Zon, J. Schofield, Symplectic algorithm for molecular dynamics simulations of rigid bodies using the exact solution of free motion, in preparation.
[16] H. Goldstein, Classical Mechanics, Addison-Wesley, Reading, Massachusetts, 1980.
[17] A.S. Rueb, Specimen inaugurale de Motu Gyratorio Corporis Rigidi, Ph.D. thesis, Utrecht, The Netherlands, 1834.
[18] C.G.J. Jacobi, Sur la rotation d'un corps, Crelle J. Reine Angew. Math. 39 (1849) 293.
[19] E.T. Whittaker, A Treatise on the Analytical Dynamics of Particles and Rigid Bodies, fourth ed., Cambridge University Press, 1937;
L.D. Landau, E.M. Lifshitz, MechanicsA Course in Theoretical Physics, third ed., vol. 1, Pergamon Press, 1976.
[20] J.E. Marsden, T.S. Ratiu, Introduction to Mechanics and Symmetry: A Basic Exposition of Classical Mechanical Systems, second ed.Texts in Applied Mathematics, Springer, New York, 2002.
[21] M. Abramowitz, I.A. Stegun, Handbook of Mathematical Functions with Formulas, Graphs, and Mathematical Tables, Dover, New York, 1965.
[22] E.T. Whittaker, G.N. Watson, A course of Modern Analysis, fourth ed., Cambridge University Press, 1927.
[23] K. Knopp, Theory of Functions: Part II: Applications and Continuation of the General Theory, Dover, Mineola, NY, 1947.
[24] M. Galassi, J. Davies, J. Theiler, B. Gough, G. Jungman, M. Booth, F. Rossi, GNU Scientific Library Reference Manual, revised second ed., Network Theory Ltd., Bristol, UK, 2005.
[25] W.H. Press, S.A. Teukolsky, W.T. Vetterling, B.P. Flannery, Numerical Recipes in C, The Art of Scientific Computing, second ed., Cambridge University Press, Cambridge, 1992.
[26] R.I. McLachlan, G.R.W. Quispel, Splitting methods, Acta Numer. (2002) 341.
[27] M.P. Allen, D.J. Tildesley, Computer Simulation of Liquids, Clarendon Press, New York, NY, USA, 1987.
[28] D.C. Rapaport, The Art of Molecular Dynamics Simulation, Cambridge University Press, Cambridge, 2004.